

TiO₂ Nanotube/CdS Hybrid Electrodes: Extraordinary Enhancement in the Inactivation of *Escherichia coli*

Steven C. Hayden,[†] Nageh K. Allam,[†] and Mostafa A. El-Sayed*

Laser Dynamics Laboratory, School of Chemistry and Biochemistry, Georgia Institute of Technology, Atlanta, Georgia 30332-0400, United States

Received August 14, 2010; E-mail: mostafa.el-sayed@chemistry.gatech.edu

Abstract: Titanium dioxide nanotubes offer distinct advantages over films of the same material in the production of hydroxyl radicals and subsequent inactivation of *Escherichia coli* in wastewater. However, their visible light absorption capabilities are limited. Semiconducting nanocrystals of cadmium sulfide have been used to increase the sensitivity of TiO₂ nanotubes to visible light. A small applied potential, using CdS-coated TiO₂ nanotube arrays, allowed for total inactivation of *E. coli* in hitherto record short time.

The use of semiconducting materials is of growing interest in a variety of fields, from energy production¹ to wastewater treatment.² It is well established in the literature that, under UV light, TiO₂ photocatalyzes the enhanced generation of OH[•] radicals, with H⁺ as a side product. This reaction is useful for a plethora of applications, including the inactivation of bacteria in wastewater treatment systems.² *Escherichia coli* is a Gram-negative bacterium that is well known for its toxicity to humans, being the cause of afflictions ranging from inflammations and peritonitis to food poisoning and urinary infections.³ This toxicity has led to the development of many strategies to disinfect various media of these organisms,⁴ and although many semiconducting materials are being tested, titanium dioxide is still among the most efficient and widely used catalysts in the disinfection of *E. coli*.⁵ Hydroxyl radicals are potent inactivators of bacteria, as they rapidly decimate the organic components of cells.⁵ However, two barriers limit the use of TiO₂ for photocatalytic inactivation of bacteria: its relatively low efficiency of light utilization due to its wide bandgap (3.0–3.2 eV) and its poor charge-transfer properties.⁵

Baram et al.⁶ have very recently reported a great enhancement in the inactivation of *E. coli* using immobilized, anodically fabricated TiO₂ nanotube (NT) arrays^{7–9} in a photocatalytic cell. The aligned porosity, crystallinity, and oriented nature of these arrays make them attractive electron percolation pathways for vectorial charge transfer between interfaces.^{10–12} Through the use of NT arrays, Baram et al. achieved an inactivation interval of less than 10 min using 25 cm² surface area NT arrays, a UV light source, and an applied bias of 3–5 V_{SEC} for bacterial solutions with a concentration on the order of 10⁶ CFU/mL *E. coli*.⁶ These results are quite promising for the use of NTs in water treatment; however, the system is still limited by the poor visible light absorption capability of the TiO₂ NTs.

More efficient visible light utilization would render this system quite attractive for disinfection procedures with sunlight as the energy source. Recent and very active research relates to the anchoring of small-bandgap nanocrystals to wide-bandgap semi-

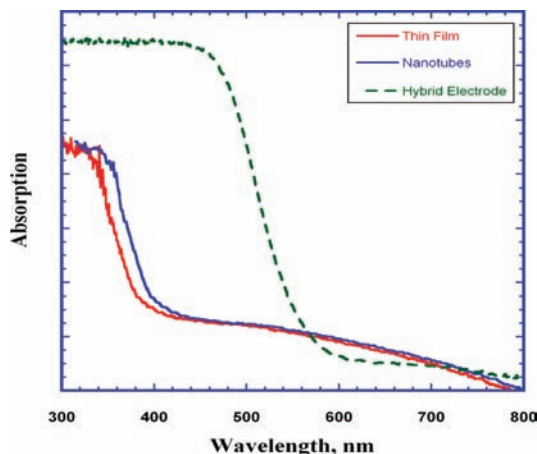


Figure 1. DRS–UV–vis spectra of the three electrodes used to inactivate *E. coli*. CdS greatly increases the visible light absorption capability of the TiO₂.

conducting metal oxides, rendering these oxides sensitive to visible light.^{13,14} Of particular interest are CdS nanocrystals, which have a relatively small bandgap and thus are capable of harvesting photons in the visible and near-infrared regions.¹⁵ The use of CdS is shown to enhance the charge carrier separation process¹⁵ and consequently is expected to enhance the inactivation efficiency. In this regard, a very complex system (Pt/CdS/TiO₂) was investigated,¹⁶ but this system suffers from the drawbacks of higher cost (from Pt) and poor charge transfer as a result of its multijunction nature and the high level of CdS coverage, which is shown in this work to adversely affect the disinfection efficiency. In the present work, we explored the capabilities of a simpler system, TiO₂/CdS hybrid electrodes, for the disinfection of water contaminated by *E. coli*. Using this hybrid system, total inactivation was achieved in less than 3 min using a small chip (1 cm²), a relatively small applied bias (0.5 V), and a white (xenon) light source.

Two sets of experiments were performed to explore the efficiency of our material to inactivate *E. coli*: photochemical (light only) and photoelectrochemical (light and applied bias). For the sake of comparison, three types of semiconductor electrodes were used in each experiment: TiO₂ thin films, TiO₂ NT arrays, and TiO₂ NT/CdS hybrid arrays (see Supporting Information for more details). In the photochemical study, electrodes were immersed in separate solutions containing *E. coli* in sulfate buffer (200 mL, 10⁷ CFU *E. coli*, 1.4 mM Na₂SO₄) under stirring and illumination from a xenon lamp (150 mW/cm²), with a water filter being used to cut-off the IR effect, and samples were collected every 10 min. For the photoelectrochemical study, a two-electrode electrochemical cell (35 mL) was used with the semiconductor material as the working electrode and Pt foil as the counter electrode under a constant applied potential of 0.5 V and illumination from a xenon lamp (150

[†] These authors contributed equally to this work.

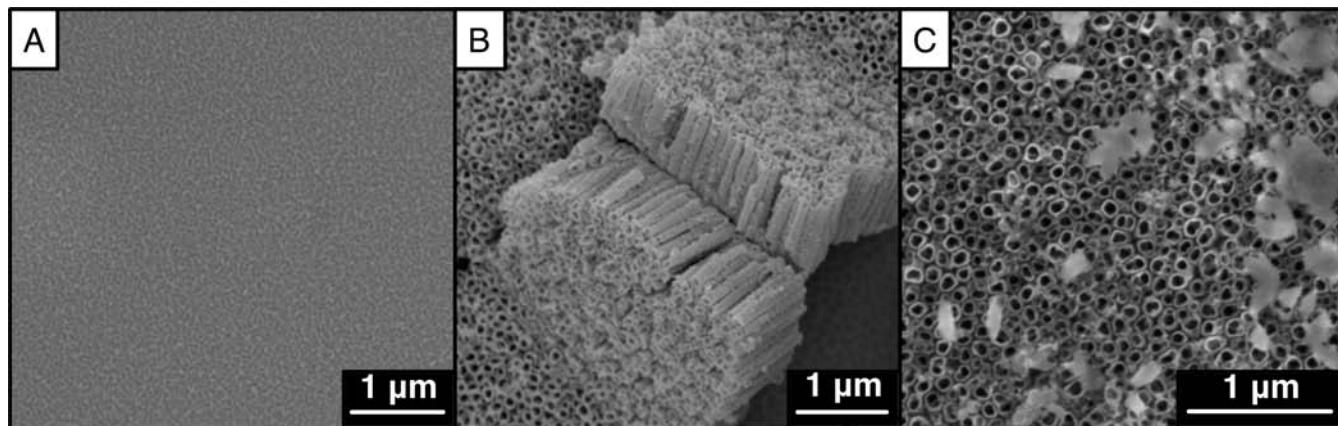


Figure 2. FESEM images of (A) titania thin film, (B) titanium dioxide nanotubes, and (C) TiO_2/CdS hybrid electrode.

mW/cm^2) (see Supporting Information for a schematic diagram of the setup used). Samples were collected every 10 min for the thin film, every 5 min for the NT array, and every 1 min for the CdS-coated NT arrays.

Figure 1 shows the diffuse reflectance spectroscopy (DRS)–UV–vis spectra of the three electrodes. Note that the absorption edge of the hybrid electrode was red-shifted (570 nm) from that of the TiO_2 thin film and NT. Given λ_g (nm) = $1240/E_g$ (eV),¹³ the estimated bandgap of the hybrid electrode is 2.17 eV, indicating the ability of the hybrid array in harvesting visible light. Figure 2 shows field emission scanning electron microscopy (FESEM) images of the three electrodes used in this study. It can be seen that the oxide film is homogeneous and covers the entire surface (Figure 2A). In the cross-sectional view of the NT arrays (Figure 2B), the tubular structure is evident, with nearly uniform wall thicknesses and NT lengths ($1.0 \pm 0.1 \mu\text{m}$). The FESEM of the hybrid electrode shows crystallites of CdS scattered on the NT surface (Figure 2C). X-ray photoelectron spectroscopy (XPS) analyses confirm the composition of the three electrodes (Figure S1, Supporting Information). The formation of titanium dioxide is evident from the O1s and Ti2p peaks, with a Ti/O molar ratio close to the stoichiometric proportion. Note that both Ti peaks, $2p_{3/2}$ and $2p_{1/2}$, are observed with a spin–orbit splitting of 5.7 eV, confirming that both signals correspond to Ti^{4+} .¹⁷ Peaks for Cd and S were also detected for the hybrid electrode.

Figure 3A shows the results obtained from the photochemical experiment; it is clear that use of the hybrid electrode led to an almost complete inactivation of *E. coli* in only 10 min without any applied bias. However, the use of both the thin film and the pure NT array led to the inactivation of only 40% and 45% of the bacteria, respectively, even after 40 min exposure under the xenon lamp. The enhanced charge transfer and light absorption capability of the hybrid electrode render it more efficient and account for the observed increase in the inactivation rate as compared to the thin film and the pure NT electrodes. Figure 3B shows the inactivation of *E. coli* in the photoelectrochemical experiment under 0.5 V applied bias, to help separate the charge carriers. It is evident that the use of the TiO_2/CdS hybrid electrode resulted in the inactivation of the *E. coli* in only 3 min. To quantify the kinetics of the inactivation process, we used the Chick model¹⁸ to estimate the inactivation rate constants (Figure S2, Supporting Information). Our estimated rate constants for the TiO_2 NTs and thin films are in very good agreement with those reported by Baram et al.,⁶ provided that lamp intensity, chip area, and current discrepancies are taken into consideration. However, our hybrid electrode showed marked inactivation rate improvements: a 1928% improvement over the

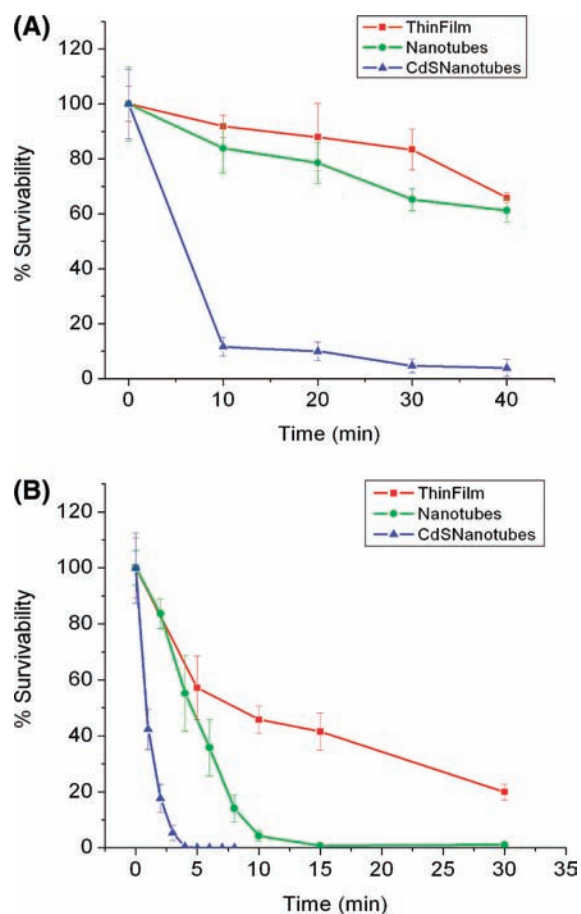


Figure 3. Inactivation of *E. coli* in photochemical (A) and photoelectrochemical (B) experiments for TiO_2 thin film (red), TiO_2 nanotube array (green), and the hybrid CdS/ TiO_2 nanotube array (blue).

thin-film electrodes and a 396% improvement over the inactivation rate displayed by the pure NT arrays (Figure 4).

We observed a relationship between the degree of CdS coverage of the NT array surface and the inactivation efficiency. When CdS was made to cover the entire surface completely (more than three layers), the chips displayed little to no inactivation ability. This is in agreement with Guijarro et al.,¹⁹ who reported a severe drop in the incident photon-to-electron conversion efficiency (IPCE) of their solar cell device when their TiO_2 surface was completely blocked from solvent contact by CdSe. The need for a sparse coverage of nanocrystals on the NT surface is both economically and environ-

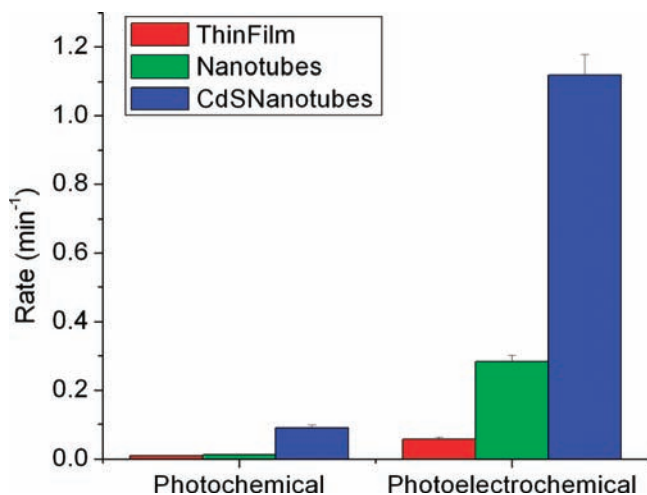


Figure 4. Rates of disinfection estimated from the Chick formula for each electrode chip under photochemical and photoelectrochemical conditions for TiO₂ thin film (red), TiO₂ nanotube array (green), and the hybrid CdS/TiO₂ nanotube array (blue).

mentally promising for the use of these types of systems in water treatment procedures.

We documented the inactivation of *E. coli* in aqueous media at a previously unattainable rate using CdS to bridge the bandgap discrepancy and render TiO₂ sensitive to visible light. The rate was shown to be even further improved upon the use of a small applied potential. This work is a step toward realizing more efficient wastewater treatment systems and has possible applications in the field of energy production. Work with other bandgap-bridging materials and with deposition procedures to more precisely control the deposited nanocrystals will further reveal the applicability of these results and is currently under way in our laboratory.

Acknowledgment. Financial support of this work by the Department of Energy, Grant No. DE-FG02-97ER14799, is greatly acknowledged. N.K.A. thanks the RAK-CAM Foundation for a postdoctoral fellowship.

Supporting Information Available: Detailed experimental procedure used to fabricate the semiconductor electrodes, as well as XPS analyses for said electrodes and graphs from which the rate constants were estimated. This material is available free of charge via the Internet at <http://pubs.acs.org>.

References

- (1) Kamat, P. V. *J. Phys. Chem. C* **2007**, *111*, 2834.
- (2) Zhang, D. Q.; Li, G. S.; Yu, J. C. *J. Mater. Chem.* **2010**, *20*, 4529.
- (3) Manning, S. A., I.; Heymann, D. *Escherichia Coli Infections (Deadly Diseases and Epidemics)*; Chelsea House Publications: New York, 2004.
- (4) Cho, M.; Kim, J.; Kim, J. Y.; Yoon, J.; Kim, J. H. *Water Res.* **2010**, *44*, 3410.
- (5) McCullagh, C.; Robertson, J. M. C.; Bahnemann, D. W.; Robertson, P. K. *J. Res. Chem. Intermed.* **2007**, *33*, 359.
- (6) Baram, N.; Starosvetsky, D.; Starosvetsky, J.; Epshtein, M.; Armon, R.; Ein-Eli, Y. *Electrochim. Acta* **2009**, *54*, 3381.
- (7) Allam, N. K.; Grimes, C. A. *Sol. Energy Mater. Sol. Cells* **2008**, *92*, 1468.
- (8) Allam, N. K.; Alamgir, F.; El-Sayed, M. A. *ACS Nano* **2010**; in press (DOI: 10.1021/nn101678n).
- (9) Allam, N. K.; Grimes, C. A. *Langmuir* **2009**, *25*, 7234.
- (10) Allam, N. K.; Shankar, K.; Grimes, C. A. *J. Mater. Chem.* **2008**, *18*, 2341.
- (11) Allam, N. K.; Shankar, K.; Grimes, C. A. *Adv. Mater.* **2008**, *20*, 3942.
- (12) Allam, N. K.; Grimes, C. A. *J. Phys. Chem. C* **2009**, *113*, 7996.
- (13) Bird, J. P. *Electron Transport in Quantum Dots*; Kluwer: Boston, 2003.
- (14) McClure, S. A.; Worfolk, B. J.; Rider, D. A.; Tucker, R. T.; Fordyce, J. A. M.; Fleischauer, M. D.; Harris, K. D.; Brett, M. J.; Buriak, J. M. *ACS Appl. Mater. Interfaces* **2010**, *2*, 219.
- (15) Baker, D. R.; Kamat, P. V. *Adv. Funct. Mater.* **2009**, *19*, 805.
- (16) Kang, Q.; Lu, Q. Z.; Liu, S. H.; Yang, L. X.; Wen, L. F.; Luo, S. L.; Cai, Q. Y. *Biomaterials* **2010**, *31*, 3317.
- (17) Allam, N. K.; El-Sayed, M. A. *J. Phys. Chem. C* **2010**, *114*, 12024.
- (18) Erkmén, O.; Dogan, C. *Food Microbiol.* **2004**, *21*, 181.
- (19) Guijarro, N.; Lana-Villarreal, T.; Mora-Sero, I.; Bisquert, J.; Gomez, R. J. *Phys. Chem. C* **2009**, *113*, 4208.

JA107034Z